DOE Award Number: DE-FG07-02ER63503

EMSP Project Number: 86729

Awardee: Washington State University

Project Title: Mechanisms of CCl_4 Retention and Slow Release in Model Porous Solids and Sediments

WSU PI: (Brent Peyton, later replaced by) Reid Miller
(509)335-4001 millerrc@wsu.edu

Lead PI: Robert Riley, Pacific Northwest National Laboratory
(509)376-1935 robert.riley@pnl.gov

EXECUTIVE SUMMARY

Results of this project provide important insights into the mechanisms by which volatile organics can be removed from porous underground environments, a vital step in the cleanup of potentially harmful contaminants found at some DOE sites. For the first time, effects of pore size and water content on the removal rates of a volatile organic have been studied independently. It has been found that the average pore size, the shape of the pores and water content all impact removal rates and ultimate cleanup levels. A relatively simple combination of two models has been found to describe contaminant removal rates from high initial organic content to small residual amounts. The data obtained and models studied can provide a partial framework for the improvement of sophisticated models of underground cleanup processes, such as vapor extraction or bioremediation.

ABSTRACT

A magnetically coupled microbalance system has been used to measure adsorption and desorption isotherms and rates of desorption for carbon tetrachloride on dry prepared porous silica particles with narrow pore size distributions in the mesoporous range. Pore size distributions estimated from the carbon tetrachloride isotherms were found to be in close agreement with those determined using standard low temperature nitrogen adsorption. Three different types of particles were studied, with average pore diameters of 2.7 nm, 4.6 nm, and 5.9 nm. Pore volumes based on carbon tetrachloride isotherms at 25 °C increased with increasing pore diameter, from (0.22 to 0.64) $cm^3\ g^{-1}$. Pore volumes based on standard nitrogen isotherms at 77 K were somewhat larger, ranging from (0.35 to 0.77) $cm^3\ g^{-1}$.

Prior to desorption rate studies, evacuated particulate samples were charged with volatile organic vapor at pressures sufficient to fill all mesopores with condensed fluid. Desorption rates into dry flowing helium were determined at 25 °C and atmospheric pressure, using the microbalance system combined with chromatographic analysis of the exit helium stream. Initial rates on the order of 1 (g CT) h^{-1} (g silica)$^{-1}$ were found to decrease to less than 1 (μg CT) h^{-1} (g silica)$^{-1}$, as mass adsorbed decreased from near 1 (g CT) (g silica)$^{-1}$ to values near 1 (mg CT) (g silica)$^{-1}$. This residual mass was desorbing at such a low rate, that it can be considered a migration resistant fraction of the original mass adsorbed. Attempts to remove this residual mass at higher temperatures were partially successful; however, differences between the microbalance and gas chromatograph responses leave open uncertainty about whether the residual mass was pure carbon tetrachloride. To date, attempts at analysis of the residual mass using solvent extraction have not removed completely this uncertainty.

For particles prepared using the same template surfactant, but with different average pore sizes, desorption rates were higher for the larger-pore particles, with correspondingly lower residual mass. Particles prepared with another template surfactant did not follow this pattern, exhibiting intermediate desorption rates and slightly lower residual mass, even though these particles had the smallest pores. These particles exhibited desorption isotherm behavior characteristic of larger pores connected by smaller openings. Except for peculiar behavior in the very early part of desorption experiments for one type of particles, the carbon tetrachloride desorption curves could be fit by a two-part model, employing a diffusion model for the bulk of the desorption, followed by a deactivation model as the mass adsorbed approached residual values.

Simultaneous microbalance and gas chromatograph measurements were used to determine carbon tetrachloride and water desorption rates from silica particles initially containing both volatile components. Varying water to carbon tetrachloride ratios were loaded on two types of particles with different pore sizes, with water always loaded first. With water on the particles, pore volumes were significantly reduced. When compared at the same mass adsorbed values, total desorption rates consistently decreased with increasing water content. Total residual mass was found to be a strong function of initial

water content, increasing nonlinearly from (1-2) mg to 15 mg, as initial water content increased from 0 % to 100 %.

As expected, during the first few hours of all desorption rate experiments, the rates of carbon tetrachloride desorption were larger than for water. At low initial water contents, total desorption rates were controlled throughout by the carbon tetrachloride rates. For higher water contents, the water rates became larger than the carbon tetrachloride rates for at least some period of intermediate times, after the bulk of the carbon tetrachloride had been desorbed. Although the compositions of the residual mass have not been independently measured, there is evidence that both components were retained, but that water was the major component when there was significant initial water on the particles.

INTRODUCTION

There is considerable interest in desorption rates for volatile organics from porous solids, relative to developing adequate models for cleanup of contaminated underground environments. It is believed that contaminant desorption rates control the overall cleanup rates and ultimate cleanup levels for most *insitu* processes. This work is part of an effort to quantify the effects of pore size, moisture content, carbon content and surface mineralization on desorption rates of volatile organics from well-characterized porous solids that are relevant to vadose zone cleanup processes. Most studies to date have been on complex soil samples, involving complicated combinations of the above factors, all of which are believed to affect desorption rates. The current approach is to study these factors one at a time, and then in combination.

In recent years, sol-gel chemical processes have been developed through which porous inorganic particles can be made with very narrow pore size distributions. This is accomplished by using surfactant template molecules around which an inorganic matrix consolidates, followed by removal of the template by calcination or extraction. By choosing production conditions and which template molecule is used, the pore size can be tuned to almost any desired value. For example, porous silica particles can be prepared with pore sizes in the mesoporous and upper microporous ranges.[1-4] Equilibrium isotherms have been measured for carbon tetrachloride on such materials, with resulting pore size distributions in good agreement with those determined by standard nitrogen adsorption analysis.[5,6] To our knowledge, no carbon tetrachloride release rate studies have been reported for such prepared particles.

Moisture can affect sorption kinetics and equilibria through competition for pore volume and surface sites, through varying solubility of organics in liquid water, and by creating barriers to transport.[7] Systematic studies have been done to characterize the effect of moisture on equilibrium isotherms.[8,9] Most prior release rate studies have been done on actual soils or soil simulants, with broad pore size distributions, and under water-saturated conditions. These studies show that a portion of the adsorbed contaminant is easily removed, whereas, a smaller portion desorbs very slowly.[10]

The amount and type of naturally occurring organic carbon can contribute significantly to adsorptive capacity of soils for volatile organic compounds, for soils with relatively high organic contents.[7,11] If the organic content is low, sorption to mineral grains likely becomes the dominant mechanism. Organic matter in soils can range from relatively recent materials, such as fulvic and humic acids, through various intermediate materials, to highly condensed organics classified as kerogen.[12] Also, it has been shown that vadose zone soils may contain significant amounts of soot particles, presumably from fires.[13] All of these materials provide strong adsorption sites for volatile organic contaminants. Humics tend to form rather loose structures, whereas highly condensed materials like kerogen form tight structures, with considerable heterogeneity. It has been postulated that it is these highly condensed, naturally occurring organics that are associated with slow sorption kinetics.[12,14] Where considerable soot particles are present, it has been found that most of the organic contaminants are associated with these particles.[13] Again, most studies have been conducted on real soils under water saturated conditions, where it is difficult to separate out effects due to moisture, pore size, and the nature and location of the naturally occurring organic materials.

Scope of the work reported here includes preparation and characterization of porous silica particles with narrow pore size distributions in the mesoporous range, followed by measurements of equilibrium isotherms and release rates for carbon tetrachloride, under dry conditions and with varying amounts of water present.

EXPERIMENTAL METHODS

Mesoporous silica particles were prepared by the method described by Zhao et al.[4] and characterized for pore size distribution, pore volume, surface area and particle size distribution. Currently, particles have been prepared containing narrow pore size distributions in the diameter range (2-6) nm.

Data are reported in the current work for three different particles, one using Tween 40 as a structure-directing template, and two using Pluronic P123 (the first at 35 °C, and the second at 35 °C followed by 80 °C, as described in Ref. 4). Herein, these particles are called T-27, P-47 and P-55, respectively, the leading letter indicating the surfactant employed in the preparation, and the numbers roughly indicating the pore size in angstroms. Standard nitrogen adsorption and desorption isotherms at 77 K were obtained for each type of particle, with pore size distributions estimated by the method of Miyata et al.[6] Sufficient carbon tetrachloride adsorption and desorption isotherm data were obtained to confirm the nitrogen results. Particle size distributions were measured in a centrifugal automatic particle size distribution analyzer.

The sorption system used in this investigation involves a magnetically coupled microbalance, designed and manufactured in Bochum, Germany. The apparatus allows careful adsorption/desorption studies over considerable ranges of temperature (-80 to +250) ºC, pressure (vacuum to 350 bar) and gas phase composition in a highly controlled environment. The microbalance is used for direct mass determination, rather than relying on PVT (pressure, volume, temperature) relationships to calculate mass adsorption or

desorption. Loads up to 60 g can be weighed in real time with a precision of 10 μg. In addition, incorporation of an Archimedes sinker in the measurement cell allows simultaneous measurement of gas phase density, which allows accurate buoyancy corrections to be made, as well as determination of equilibrium gas phase compositions for binary gas mixtures. The system is computer controlled, making it ideal for measurements on systems with long equilibrium times, or for long-term release rate studies. This same microbalance system was used in a prior study of densities and dew points of selected hydrocarbon mixtures,[15] by employing it as a dual-sinker densimeter instead of a sorption/density measurement system.

A schematic diagram of the sorption system is shown in Fig. 1. A sample holder has been designed to contain fine porous particles in multiple thin beds (four beds, each 16 mm diameter, with sample loaded 2-3 mm deep). This holder is suspended in a cell, with a coupling housing above it, of (100 ± 5) cm^3 total free volume. The cell and coupling housing are maintained at any desired temperature within ± 0.01 ºC by fluid (from a constant temperature circulator) flowing through metal jackets surrounding these elements (not shown in Fig. 1). Both the cell and the coupling housing are insulated on the outside.

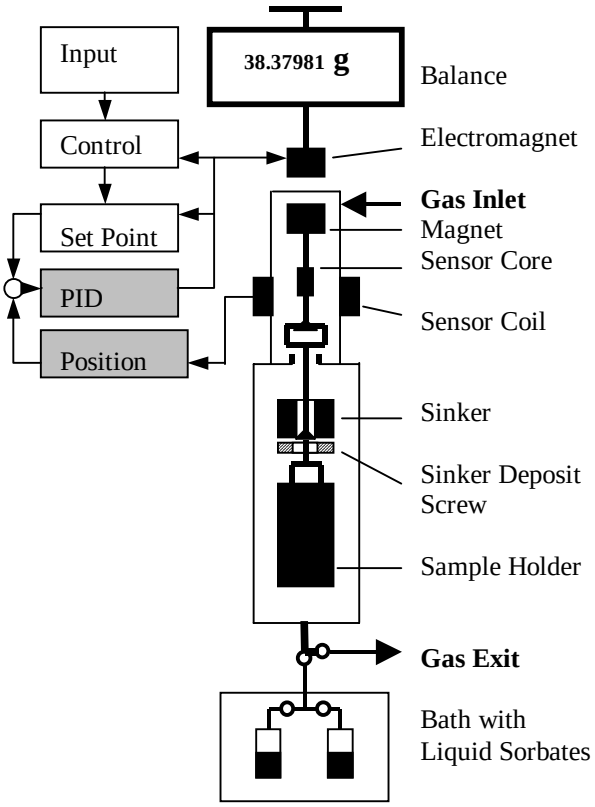

Figure 1. Schematic Diagram of the Sorption/Density Microbalance System

Cell temperatures are measured by calibrated platinum resistance thermometry, with accuracy better than 0.1 °C. Cell pressures are determined to 0.0001 bar by a quartz spiral gauge (up to 11 bar).

The true mass m_H^{true} and volume V_H of the sample holder have been determined as the intercept and slope of microbalance mass measurements of the sample holder versus helium (99.999 % minimum purity) gas density, from vacuum to 10 bar. Helium densities were taken from AllProps.[16] Similar measurements of the sample holder loaded with a porous solid yield the true mass m_{H+S}^{true} and solid volume V_{H+S} of the holder and sample combined. The true mass and volume of the sample can be obtained by difference:

$$\begin{aligned} m_S^{true} &= m_{H+S}^{true} - m_H^{true} \\ V_S &= V_{H+S} - V_H \end{aligned} \tag{1}$$

The volumes are determined at the temperature desired for sorption measurements. The inherent assumption in these calibrations is that helium does not adsorb in significant amounts. If it does, the measured V_{H+S} term will be too small (by a factor proportional to the Henry's law constant for helium adsorption). The net effect will be that all sorption measurements are relative to helium, which is considered standard practice.[17]
As mentioned above, the cell contains an Archimedes sinker, whose true mass m_{AS}^{true}, volume V_{AS}, and thermal expansion coefficient have been independently determined. This sinker can be weighed separately from the sample holder, and Archimedes sinker apparent mass m_{AS}^{app} is used to determine density of the gas phase in the cell.

$$\rho = \frac{m_{AS}^{true} - m_{AS}^{app}}{V_{AS}} \tag{2}$$

After the prepared and dried porous particles are loaded into the sample holder, the holder plus sample is dried in an oven at 150 °C for at least 12 h and then transferred to a desiccator for cooling. The sample holder is loaded into the microbalance cell under flowing helium and the cell quickly sealed onto the system. The cell is then evacuated at 70 °C for at least 12 h and then cooled to the desired operating temperature. Long evacuations at low temperatures are avoided, since particles slowly gain mass, presumably from outgassing of other parts of the system.

Carbon tetrachloride (CT) vapor is allowed to fill the gas space in the cell. A valve is opened between the cell and a dried and degassed liquid CT sample (99.9 % minimum purity), kept in a metal vessel in a separate constant temperature bath (Fig. 1). By adjusting the temperature of the liquid sample, thus changing its vapor pressure, pressures in the cell can be independently varied as desired to study adsorption and desorption isotherms. This sample loading method is similar to that reported in a study of sorption of volatile organics in heavy liquid polymers.[18] A second line from the cell to a degassed

liquid water sample (nanopure, 18 MΩ-cm resistivity), also contained in the separate constant temperature bath, can be used to load water on the porous solid, to study competitive water + CT sorption phenomena.

As the gas adsorbs on the porous solid, holder plus sample apparent mass m_{H+S}^{app} and sinker mass are recorded versus time, until equilibrium is obtained. The vapor density in the cell is determined from the sinker mass, using Eq. 2. At any time, the total mass adsorbed m^{ad} is calculated from the following equation:

$$m^{ad} = \frac{m_{H+S}^{app} - m_{H+S}^{true} + \rho V_{H+S}}{\left(1 - \rho / \rho_{AP}\right)} \qquad (3)$$

The last term in the numerator is a correction for buoyancy of the holder plus solid sample. For the current work, this term is nearly negligible for component isotherm measurements and a nearly constant correction of about 1 mg for desorption rate experiments. The denominator term is a correction for buoyancy of the adsorbed phase, involving the density of the adsorbed phase ρ_{AP}, which is estimated as the liquid density of the adsorbate. Fortunately, this correction is unimportant for sorption work at low cell pressures, as reported in this investigation.
To charge the particles with both water and CT, the particles are exposed to water vapor first. Mass of water adsorbed is calculated using Eq. 3. Mass of water in the gas phase can be based on measured density (Eq. 2) and cell volume, or the density can be closely estimated using the ideal gas law based on the measured pressure in the cell. After addition of CT at higher pressure, the new measured gas phase density is used to estimate the composition of the gas phase. Coupled with the known total mass of water in the system, and the new measured total mass adsorbed, mass of each component in both the gas and adsorbed phases can be calculated. Further details of these calculations can be found elsewhere.[19] For all mixtures studied here, the mass of CT in the vapor phase was (33-34) mg, and the mass of water in the vapor phase (1-2) mg, after loading both species on the particles. Corresponding total masses on the particles were (140-290) mg.

A typical procedure for measurements of pure CT isotherms is as follows. Adsorbent (0.5-1.0 g) is loaded into the sample holder and placed into the microbalance cell and evacuated at elevated temperature, as described above. Helium is introduced at various pressures in the range (0-10) bar, to determine the true mass and volume of the sample plus holder. CT is introduced at a pressure just below saturation at the cell temperature. A series of equilibrium measurements are made of mass adsorbed (from Eq. 3) versus CT pressure, by incrementally lowering the bath temperature for the liquid CT sample (or by withdrawing CT vapors into the cold trap in the vacuum system). The valve between the liquid sample and the cell is always closed for the final approach to equilibrium at each point. Apparent mass and system pressure are followed versus time to determine when equilibrium has been attained. Equilibrium measurements of mass adsorbed are believed accurate to better than 1 mg/g. Typical times to equilibrium are in the range of 30-90 min, for accuracies at this level. After desorption measurements are completed, CT pressure is incrementally increased to determine the adsorption isotherm. At the end

of this procedure, the adsorbent is again fully loaded, at a CT pressure near saturation at cell temperature.

For desorption rate studies (called sweep experiments) involving pure CT, the typical starting point is an equilibrium point on the adsorption isotherm at a CT pressure sufficient to fill all pores, but still well below the CT saturation pressure at the cell temperature. For rate studies involving both CT and water, the water is loaded first to the desired mass adsorbed, followed by equilibrium adsorption of CT at a pressure below saturation, with the cell isolated from the liquid CT source. Helium (99.999 % minimum purity) is used as a sweep gas. It is introduced to the cell to bring the pressure to just above atmospheric, the exit valve is opened, and sweep gas flow started immediately. Flow rate is controlled at 30.0 cm^3/min by a mass flow controller. This rate is sufficient to rapidly sweep the vapor space in the 100 cm^3 cell, but small enough so that drag corrections on the sinker and sample holder are small. Apparent mass and sinker mass are followed versus time, with small corrections applied for sweep gas drag, so that mass adsorbed (from Eq. 3) versus time can be determined.

The entire process of microbalance measurements is under computer control, allowing sample mass to be measured at any desired time intervals, with periodic measurements of zero point (load disengaged) and sinker mass. Corrections for zero-point drift are made. The balance is automatically calibrated against internal standards at fixed intervals, and appropriate corrections are made for changes in air buoyancy on the internal calibration masses due to changes in room air density. All of this allows operation over very long periods of time, with accuracies for mass measurements approaching 20 μg.

For sweep experiments, when the rates of desorption drop significantly below 10 μg/h, uncertainties in the rates become large when slopes are extracted from the mass adsorbed versus time data from the microbalance. These rates can be followed to below 0.1 μg/h by measuring the CT concentrations in the exit gas from the cell.

The outlet gas from the cell is continuously sent to the sample loop of a gas chromatograph (GC) equipped with both a flame ionization detector (FID) and an electron capture detector (ECD). The FID is used to measure CT concentrations from (1-50,000) ppm, and the ECD for CT concentrations from (0.01-1) ppm. Calibration was accomplished using dilutions of a certified standard of (1010±20) ppm CT for concentrations below the level of the standard, and by using liquid CT (99.9 % minimum purity) evaporated into air and held in heated cylinders for higher concentrations. Total estimated uncertainties[19] in the GC sampling and measurements are ±10 % for concentrations below 5000 ppm, increasing to near ±20 % at 50,000 ppm.

Another reason to measure exit CT concentrations is to follow simultaneous release of CT and water, with water rates determined as the difference between the total mass desorption rate (from the slope of the microbalance mass adsorbed versus time data) and the CT rate (from the exit gas CT concentration measurements, combined with the sweep gas flow rate). There were two problems that had to be overcome to produce meaningful data. First, the initial gas phase contained (33-34) mg of CT, which was swept out of the

cell along with the CT released from the solid sample. This was accounted for by performing a series of blank runs with the empty sample holder in the cell, and using the measured empty holder CT concentration versus time data to correct the results for runs with particles present. Greatest uncertainties in this procedure are at the start of a sweep, when a large fraction of the exit CT is coming from the gas phase. At sweep times greater than 20 min, less than 2 % of the CT exiting the cell was from the initial gas phase.

The second major issue is that care must be taken in the early stages of the sweep experiments to reconcile times for the GC samples with those for the microbalance readings. Uncertainties due to this issue cannot be completely eliminated. When they are combined with the large GC uncertainties associated with the early high CT concentrations in the exit gas, and the uncertainties in the early corrections for the gas-phase CT discussed above, the combined uncertainties in measured CT desorption rates during the first few minutes of a run are exceptionally large, perhaps exceeding 100 % for the first few minutes of a sweep. Since water desorption rates are calculated as the difference between the total desorption rates and the CT desorption rates, the values for this quantity are highly uncertain as well during this brief initial period. Further discussion of the details of these uncertainties can be found in Reference 19.

RESULTS AND DISCUSSION

From preliminary microbalance measurements on a commercial silica gel, as well as on several prepared mesoporous silica samples available in the early stages of this project, the following conclusions were reached.[20-22]

1) Pore size distributions measured near room temperature using CT isotherms in the current apparatus are in excellent agreement with those obtained from standard nitrogen sorption techniques, using the same method of calculation, in agreement with the literature.[5]
2) CT desorption rates are nearly independent of the sweep gas used (air or helium), and not much different from directly evacuated samples.
3) CT desorption rates are usually larger for larger pore samples, when compared at the same CT mass adsorbed values.
4) Residual mass (on the order of 1 mg per g of silica) is always found after CT desorption experiments at 25 °C, with at least partial reduction possible by increasing temperature to 85 °C.

These studies provided the foundation for a more systematic investigation of the effects of pore size on CT desorption rates and residual mass, and on the impact of water on these phenomena. The results are described below in three sections.

Particle Characterization: Isotherms

Zhao et al.[4] reported mesophase structures, surface areas, pore sizes and pore volumes for the particles they prepared by the methods adopted for the current study, as shown in

Table 1. The Ref. 4 pore diameters represent peak pore sizes, and they were calculated from the adsorption branch of standard nitrogen isotherms using the BJH method. For the current work, pore diameters are from the adsorption branch of standard nitrogen isotherms using the method of Miyata et al.[6], which is found to yield pore sizes (0.5-0.7) nm larger than the BJH method for these particles.

Table 1. Mesophase structure, peak pore diameters (D), BET surface areas (SA) and pore volumes (V) from Ref. 4, compared with properties from the current work.

		Properties from Ref. 4			This Work		
Particles	Structure	D/nm	SA/m2 g-1	V/cm3 g-1	D/nm	SA/m2 g-1	V/cm3 g-1
T-27	cubic	2.0	700	0.36	2.7	700	0.39
P-47	hexagonal	4.7	690	0.56	4.3	520	0.35
P-55	hexagonal	6.0	780	0.80	6.3	760	0.77

Detailed nitrogen adsorption and desorption isotherms for the particles used in the current work are presented in Fig. 2. All isotherms are Type IV (IUPAC classification), with varying hysteresis behavior. For T-27 particles, behavior is Type H1, but with no visible hysteresis for filling the majority of mesopores. There is a narrow loop at higher relative pressures of Type H4, which has been reported for some highly-ordered bicontinuous cubic pore systems,[8] and has been interpreted as particles with larger pores connected by smaller openings.[23] Both adsorption and desorption branches yield a peak pore diameter near 2.7 nm, with the desorption branch indicative of a small secondary peak at 4.6 nm. Limited carbon tetrachloride isotherm data show a very narrow but visible hysteresis for mesopore filling, and these data are in accord with the narrow loop at higher relative pressures. Peak pore sizes from the nitrogen data are closely reproduced by the carbon tetrachloride data.[19,20]

A major hysteresis loop is obvious for the P-47 particles, with the shape characteristic of Type H2 hysteresis. Both adsorption and desorption branches yield a single peak for the pore size distribution at 4.3 nm, if the cylindrical form of the modified Kelvin equation is used instead of the spherical form for the analysis of the adsorption branch (not done in Ref. 24). This is a necessary modification of the Miyata et al.[6] method for larger pores with significant hysteresis, if reasonable agreement is to be obtained between analyses of the two branches of an isotherm. The shape of the adsorption and desorption isotherms and the corresponding pore-size distributions are closely reproduced by current carbon tetrachloride isotherm data.

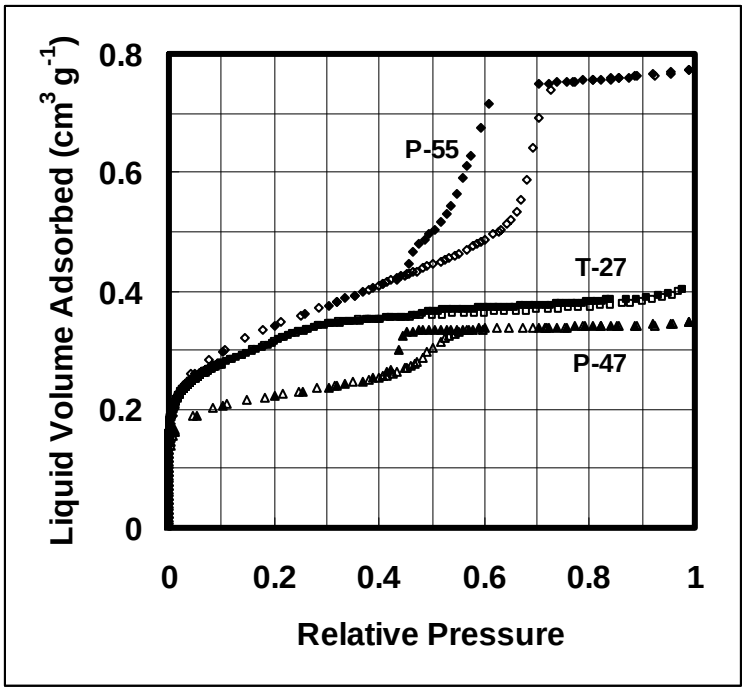

Figure 2. Standard nitrogen isotherms for T-27, P-47 and P-55 particles: adsorption (open symbols) and desorption (closed symbols).

The P-55 particles exhibit a wide hysteresis loop, with the shape characteristic of Type H1 hysteresis. An interpretation of the differences in hysteresis behavior between the P-47 and P-55 particles is that the P-55 particles have less pore-blocking.[23] Peak pore sizes predicted from the adsorption and desorption branches are 6.3 nm and 5.8 nm, respectively. Also, the desorption branch for the P-55 particles exhibits some H3 behavior at the lower closure of the hysteresis loop. This results in a small secondary peak at 4.3 nm. Again, the limited carbon tetrachloride isotherm data taken are consistent with these findings from the nitrogen isotherms, although not sufficient to confirm the details of the H3 behavior.

Peak pore sizes (from the adsorption branch), total pore volumes and BET surface areas from the nitrogen sorption experiments are compared with the Ref. 4 data in Table 1. The method of Miyata et al.[6] yields larger pore diameters than the traditional BJH method, so agreement is believed to be close for the T-27 and P-55 particles. The P-47 particles used in the current work appear to have somewhat smaller pores than those of Ref. 4. The pore volumes and surface areas for T-27 and P-55 agree with the values from Ref. 4, however, both properties are considerably smaller for the P-47 particles in the current work.

Corresponding pore volumes from the carbon tetrachloride isotherms are smaller than those determined from the nitrogen isotherms: T-27 (0.22 cm^3/g); P-47(0.29 cm^3/g); P-55(0.64 cm^3/g). A possible explanation of these smaller CT pore volumes is that because

of their larger size CT molecules can not fill as many of the smallest pores. The T-27 particles were found to have the largest ratio of micro-pore volume to meso-pore volume, based on the nitrogen isotherms,[24] and these particles exhibit the largest difference between nitrogen and CT pore volumes. Other explanations could be that the use of bulk liquid densities is inappropriate to translate between mass adsorbed and pore volumes, or that there are structural differences at the vastly different temperatures employed in the measurement of these nitrogen and CT isotherms, resulting in an appreciable change in pore volume. The modest reversal in relative pore volumes for the T-27 and P-47 particles should be noted.

A particle size distribution analyzer was used to measure overall particle sizes for each type of particle. Average particle diameters are found to be near 20 μm for the T-27 particles and about 4 μm for the P-47 and P-55 particles.

Pure CT Desorption Experiments

Duplicate CT desorption rate experiments (sweep experiments) have been performed at 25.0 °C and near atmospheric pressure (0.93 bar) on each of the three types of particles: T-27, P-47 and P-55. Helium gas flowing through the 100 cm^3 cell at a rate of 30.0 cm^3/min was used to carry the desorbed CT out of the system. Microbalance measurements of mass adsorbed versus time were made throughout the runs, with GC measurements of the exit gas stream during the later stages to accurately determine desorption rates below the limits of the microbalance. Agreement between the duplicates was good, nearly within the ability to read the graphs, so selected runs involving the most complete data sets are presented below. More complete graphical data can be found elsewhere.[24]

The most fundamental measurements from the microbalance are mass adsorbed versus time data. Since GC measurements yield desorption rates, GC mass adsorbed values are based on the mass adsorbed value from the microbalance corresponding with the last GC point taken before the microbalance rates reach the detection limit or are terminated for other reasons. Other GC mass adsorbed points are calculated by integration of the GC rate versus time curve.

Microbalance (MB) and GC mass adsorbed versus time data for all three particles are shown in Fig. 3. Note that all mass adsorbed values and rates are reported per unit mass of particles. The MB curves are distinguished by the GC points with which they most closely agree. Early desorption rates (slopes of the curves) are higher, approach to equilibrium is faster, and residual mass is lower for the larger pore size P-55 particles, compared with the smaller pore size P-47 particles, as one might expect. However, the desorption rates appear to be intermediate for the T-27 particles, and the residual mass is even lower than for either P-47 or P-55, neither observation being expected for particles with the smallest pore size. The implication is that differences in the particulate pore structures, which depend on the preparation method, can be as important as modest pore size differences in determining relative desorption rates and residual masses.

The concurrence of the MB and GC curves over a long time span for the T-27 particles indicates that the major component being released at 25 °C was CT. The last five GC points for T-27 were taken after raising the cell temperature to 85 °C. This resulted in a 20 % reduction in residual mass (from 1.2 mg/g to 1.0 mg/g), measurable as CT by integration of the GC rates. In contrast, the MB values of mass adsorbed decreased by 53 % (from 1.2 mg/g to 0.56 mg/g) over the same time period.

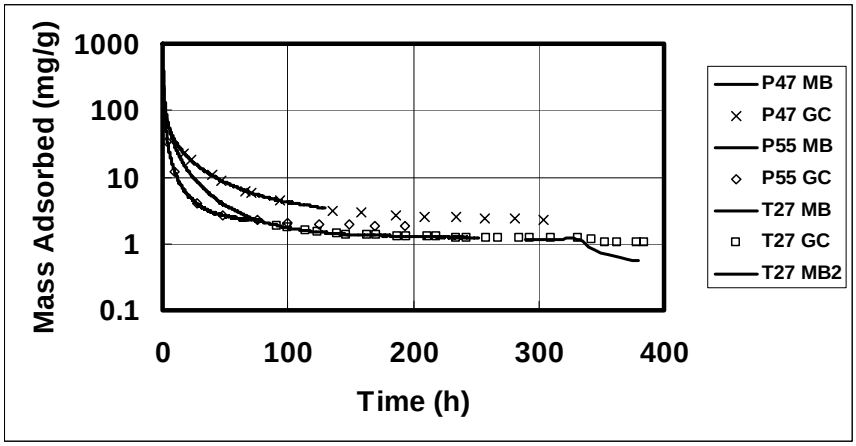

Figure 3. Mass adsorbed versus time from microbalance (MB) and gas chromatograph (GC) readings for pure CT desorption rate experiments.

There are some possible explanations for these differences. It is possible that an initial very large amount of CT coming off the particles was missed before the first GC sample was taken. Another factor may be that some of the CT released from the particles is being re-adsorbed elsewhere in the experimental system, rather than passing to the GC. Finally, it may be that the residual mass is not all CT. There is fairly strong support for the first of these possible contributions. The temperature set point was changed at 333 h, and it required only one hour for the cell temperature to increase from 25 °C to 85 °C. The next GC point was taken at 342 h. During this time, the MB mass adsorbed values decreased by 0.4 mg/g. Thus, at least one third of the initial residual mass was desorbed prior to the first GC measurement, and any CT it contained was missed in the GC measurements. If this mass released was all CT, it would account for the differences between the MB and GC values at the end of the run. The apparent rather gradual divergence of the GC and MB mass adsorbed versus time curves at 85 °C would lend support for the other possible reasons, partial re-absorption in the system or a component of the residual mass being something other than CT.

Plots of desorption rate versus time from the same runs are shown in Fig. 4. The GC rates are in excellent agreement with the MB rates (determined by taking slopes of the MB data), and the GC rates extend smoothly in time to values approaching 0.0001 mg/h/g. It should be noted that these are independent measures of CT release rates and there is no forced agreement of the rate versus time data from these two sources. MB rates become unstable at values below 0.005 mg/h/g, as shown for the T-27

particles. The intermediate rate values for T-27 at times from (2-200) h are clearly shown on this figure. It is interesting to note that the desorption rates for the P-55 particles are lower than those for the P-47 particles for times beyond 2 h, as the larger pore particles more quickly loose the bulk of their very large initial CT charge and more rapidly approach residual mass adsorbed.

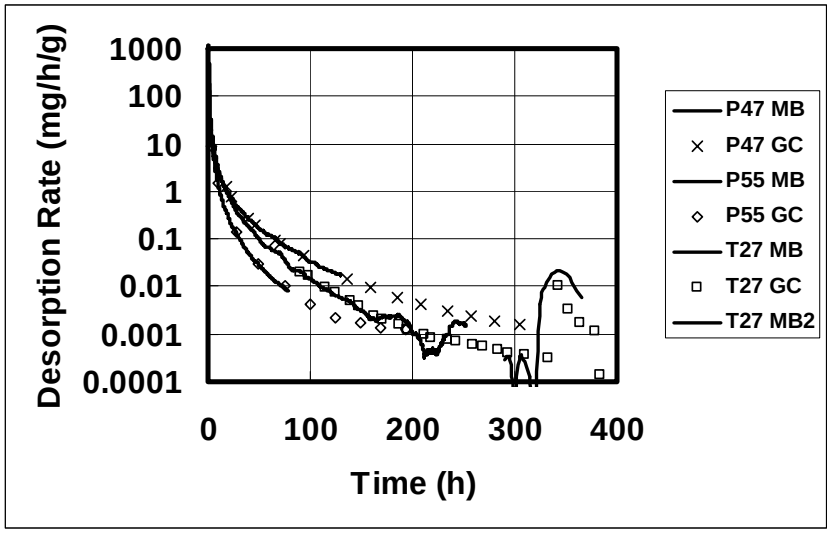

Figure 4. Desorption rate versus time from microbalance (MB) and gas chromatograph (GC) readings for pure CT desorption rate experiments.

The impact of changing the cell temperature from 25 °C to 85 °C is clearly shown on Fig. 4. The GC desorption rate jumped by a factor of 20 to 0.01 mg/h/g, then decreased to values of the same order as before the temperature change. This behavior is roughly confirmed by the microbalance rate, which jumped from unsteady values below 0.001 mg/h/g before the temperature change, to steady values near 0.02 mg/h/g at (340 to 350) h, then dropped steadily to a value of 0.006 at 365 h, then became unsteady again as the rate dropped further with time. Comparable results were observed in other measurements,[22] where a two-stage temperature increase was applied at the end of a desorption run on prepared particles with similar pore size and residual mass to the T-27 particles. The GC and MB rate curves for the first increase (to 68 °C) were very similar to those on Fig. 4. For the second increase (to 87 °C), the MB rate curve again increased to a maximum near 0.02 mg/h/g. The GC curve mirrored this increase, but it remained an order of magnitude lower. This observation would favor the theory of another component in the residual mass besides CT.

Desorption rate versus mass adsorbed curves are shown for all three particles on Fig. 5. The initial mass adsorbed was near 400 mg/g for the P-47 and T-27 particles, but was 1000 mg/g for the larger pore volume P-55 particles. Compared at the same mass adsorbed values, rates for the P-55 particles are about a factor of four higher than for the P-47 particles, except for the very early period where the mass adsorbed is above 100 mg/g. Rates are intermediate for the T-27 particles for mass adsorbed values from near 100 mg/g down to about 3 mg/g. Below this value, the rates for the T-27 particles

become higher than for the other particles, as required for a smaller residual mass. Data for the high temperature part of the T-27 run are not shown, as they add little insight to the discussion based on the prior figures.

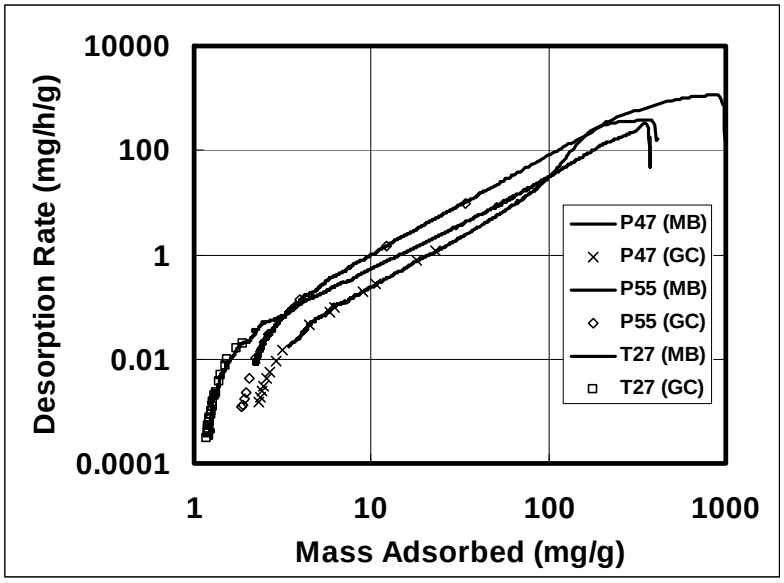

Figure 5. Desorption rate versus mass adsorbed from microbalance (MB) and gas chromatograph (GC) readings for pure CT desorption rate experiments.

The excellent agreement between the microbalance and gas chromatograph measurements indicates that the vast majority of the material being released by the particles is CT, down to residual mass levels. What is not so certain is the nature of the residual mass. Solvent extraction techniques have been used in an attempt to determine the composition of the residual mass subsequent to desorption runs. Multiple accelerated hexane solvent extractions at 60 °C and 1500 psi have been used, in conjunction with liquid GC analysis, to determine the maximum amount of CT extractable from the spent particles. Amounts extractable as CT (using multiple extractions) are about 20 % of the residual mass for P-47 and about 10 % for P-55. Estimates of total extractable CT (based on single extractions) are about 25 % for T-27. It has not been possible to calibrate percent recovery for this technique, so it is not known if these numbers represent all CT present or only some fraction thereof. A technique involving dissolving the spent particles in concentrated caustic prior to extraction is being investigated.

It has been possible to fit the mass adsorbed versus time curves of Fig. 3 in two parts, by employing a spherical diffusion model[25] for the bulk of the desorption process and a deactivation model[26] at low mass adsorbed (approaching residual mass values). The former produces a straight-line region on Fig. 5, while the latter follows the curvature to residual mass values. These models do not account for curvature at high mass adsorbed, consistently observed for the P-47 particles. More details on these calculations can be found elsewhere.[24]

Water + CT Desorption Experiments

Systematic studies of the effect of water on desorption rates and residual mass values have been conducted for T-27 and P-47 particles. In each experiment involving water, the water was added to the particles first, followed by CT addition at sufficient gas phase pressure to fill the mesopores.

For T-27 particles, desorption rate experiments were run at 25 °C and atmospheric pressure with 19 wt%, 34 wt% and 100 wt% initial water concentrations on the particles, using helium as the sweep gas at the same rate as for the pure CT desorption experiments described above. For P-47 particles, desorption rate experiments were conducted at the same conditions, for water contents of 12 wt%, 45 wt% and 100 wt%.

Microbalance (MB) total mass adsorbed versus time curves are shown in Figs. 6-7, including pure CT data (0 wt% water). GC results are shown for pure CT only, since only in this case do they represent total quantities. Total residual mass increases nonlinearly with increasing water content, from (1-2) mg/g for pure CT to about 15 mg/g for pure water. For pure water, the residual mass is on the order of 10 % of the initial mass charged, whereas, for pure CT it is less than 0.5 %. Since water was added first in all experiments, the implication is that CT has some impact on how tightly water is held to the particles. This will be explored below when individual component rates are presented and discussed.

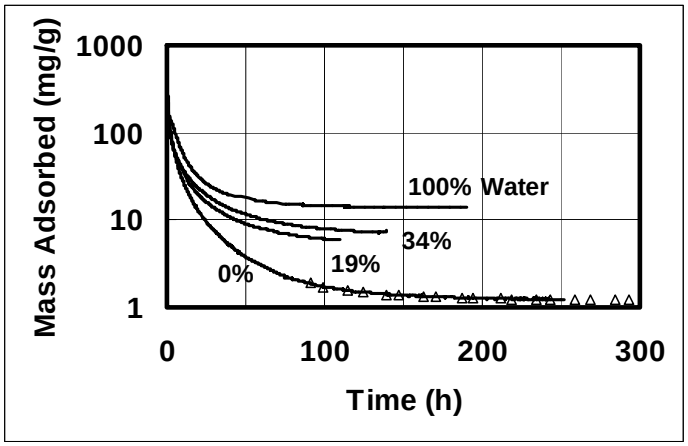

Figure 6. Total mass adsorbed versus time from microbalance readings for water + CT desorption rate experiments on T-27 particles.

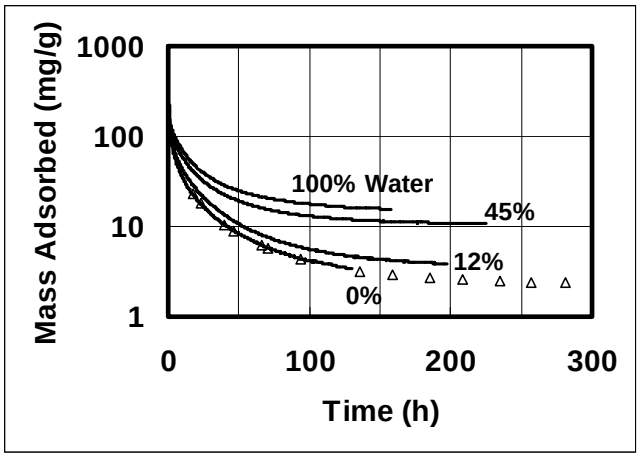

Figure 7. Total mass adsorbed versus time from microbalance readings for water + CT desorption rate experiments on P-47 particles.

Total desorption rate (from slopes of MB readings) versus total mass adsorbed curves are shown on Figs. 8-9. Note the systematic, nonlinear reduction in initial mass adsorbed with increasing water content. On a volumetric basis, the reduction in capacity between pure CT and pure water was 16 % for T-27 particles and 36 % for P-47 particles. For each type of particle, the curves for all three experiments with CT present are almost identical during the early stages of the runs (high mass adsorbed). As CT was charged last and is more volatile than water, the bulk of the material coming off the particles should be CT in this region. Below mass adsorbed of (100-200) mg/g, these three curves fan out, with the higher concentration of water curve close to the pure water curve for a mid-range of mass adsorbed values. At mass adsorbed values below (30-50) mg/g, the curves all diverge, accommodating the spread of residual masses.

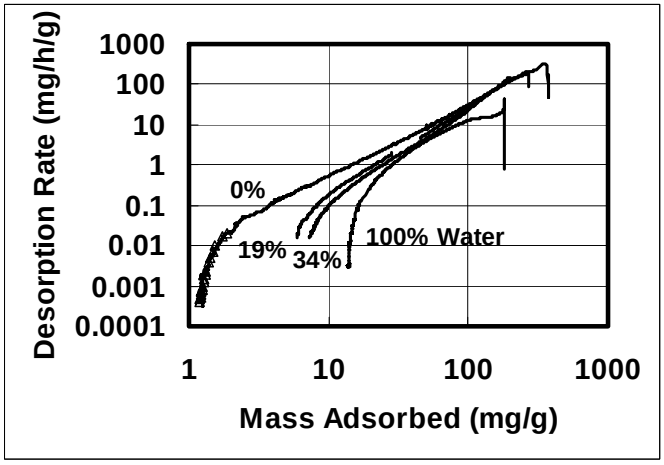

Figure 8. Total desorption rate versus total mass adsorbed from microbalance readings for water + CT desorption rate experiments on T-27 particles.

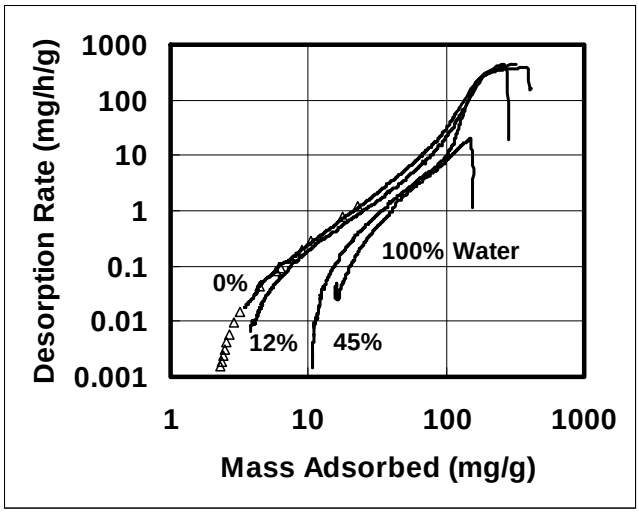

Figure 9. Total desorption rate versus total mass adsorbed from microbalance readings for water + CT desorption rate experiments on P-47 particles.

MB total desorption rate versus time curves (not presented here but available elsewhere[19]) are very similar for all experiments involving water on both types of particles. Pure CT curves for these two particles exhibit the largest differences (see Fig. 4), with rates for T-27 particles lower than those for P-47 particles throughout the sweep. Similar but smaller differences seem to exist for the water + CT mixtures, whereas, the pure water rate versus time curves are almost identical. The small differences in total rate versus time curves form a systematic pattern with initial water content. During the early stages (small values of time), the rates for pure CT are the highest and the rates for pure water the lowest. There is a cross-over point at about 10 h for the T-27 particles, and at about 20 h for the P-47 particles, with the rates for pure water the highest and the rates for pure CT the lowest for the remainder of the sweep experiments.

GC samples were taken throughout the desorption rate experiments involving water + CT, so that the total desorption rates could be resolved into separate CT and water rates. The GC results give the CT rates directly, while the water rates are calculated as the MB total rates minus the CT rates. For the experiments with the lower initial water content on each type of particle, CT rates were found to dominate the total rates throughout.

The results for the higher water content runs on each type of particle are more interesting. For T-27 particles loaded with 34 wt% water, individual component and total desorption rate curves are shown on Fig. 10. CT desorption rates dominate the total rate at both small values of time and at long times. There is an intermediate range of time (from 5 h to 40 h) when the water desorption rates are actually higher than the CT desorption rates. This is consistent with a physical picture of the bulk of the CT coming off first, followed by the bulk of the water. At long times, water has neared its residual mass adsorbed, and the total rate is again controlled by the slow CT release rates.

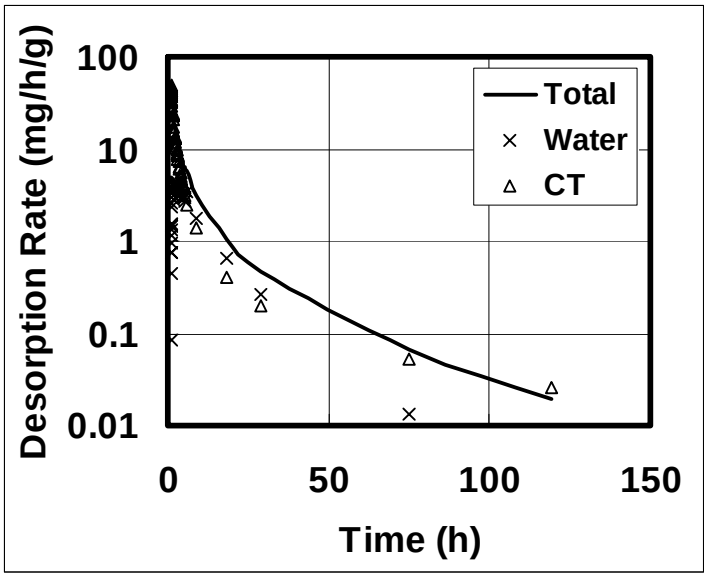

Figure 10. Desorption rates (total, water and CT) versus time for the sweep experiment involving 34 wt% water on T-27 particles.

Results for P-47 particles loaded with 45 wt% water show an even more dramatic two-stage desorption process. The rate curves are shown on Fig. 11 for the entire run. Other than the very early part of this experiment, the water desorption rates are much larger than the CT desorption rates, although they seem to be converging when the run was terminated at 220 h. Thus, one could guess that there may be another cross-over at longer times, with the slow CT release rates eventually dominating.

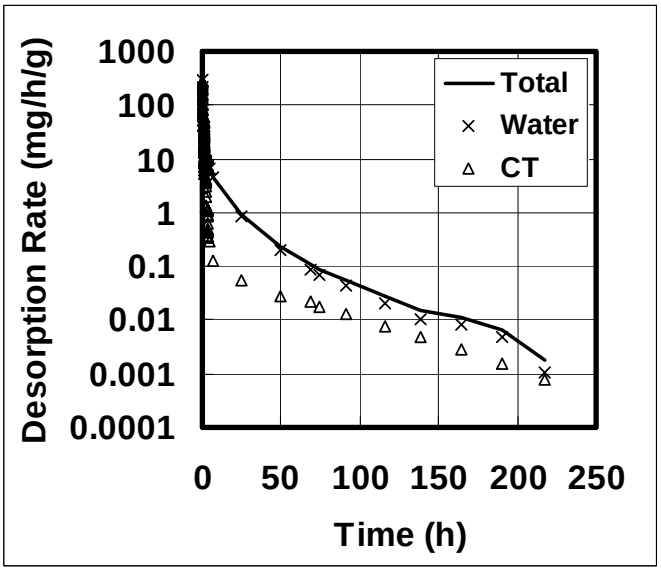

Figure 11. Desorption rates (total, water and CT) versus time for the sweep experiment involving 45 wt% water on P-47 particles.

The results for the first four hours of this run are shown on Fig. 12. The first two or three points indicate relatively high water rates, but these points have very high uncertainty due to the issues discussed in the experimental section above, and they are probably spurious. There is no reason to believe that the initial release rates should be higher in water content than the initial gas phase in the cell, which was estimated to contain 33 g CT and 2 g water for this experiment. Ignoring the first few points, the CT rates are larger than the water rates, up to 1.2 h. Then, there is a cross-over, with the water rates becoming larger, and, beyond 2 h, the water rates dominate the total desorption rates.

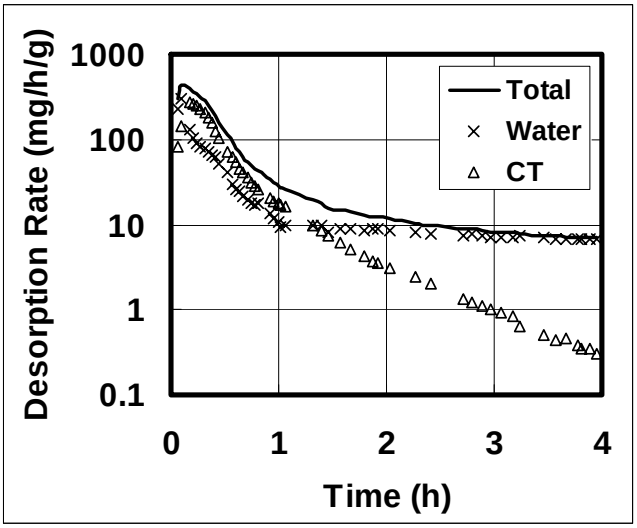

Figure 12. Desorption rates (total, water and CT) versus time for the first four hours of the sweep experiment involving 45 wt% water on P-47 particles.

The very large uncertainties in the data for the first few minutes of a sweep experiment, when desorption rates are extremely high, preclude accurate estimates of the composition of the residual mass through integration of the component rate versus time curves. For example, using the high initial water rates indicated on Fig. 12 for the first few minutes of the sweep experiment, residual mass for water is predicted to be negative, and residual mass for CT is predicted to be much larger than the total residual mass from the MB readings. However, if one makes the assumption that the total releases from the particles (MB rates) during the first 20 min of the experiment discussed above (Figs. 11-12) are pure CT, then reasonable estimates result for mass adsorbed of each component versus time, using actual data from 20 min onward. With this calculational method, the mass adsorbed versus time curves of Fig. 13 were produced.

This method is justified on the following arguments. Since CT was added last to the particles, and is significantly more volatile, the initial releases from the particles should be predominately CT. Thus, the initial CT to water ratio of exit rates, which should be approximated by the initial gas-phase ratio of CT to water of 33:2 on a mass basis, should very rapidly increase to negligible water exit rates. At 20 min, the effect of the initial gas phase CT on the CT exit rates has dropped to less than 2 %, and the problems of matching the GC measurements to the MB data have eased somewhat. Thus, this seems

a reasonable point to switch back to the calculations based on the actual measurements. It should be noted, however, that the long-time values of component masses adsorbed on Fig. 13 are somewhat sensitive to the switch-over time chosen.

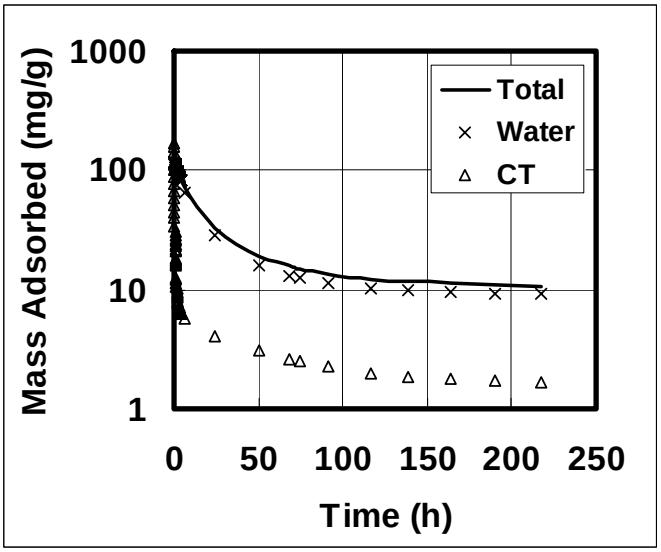

Figure 13. Estimated mass adsorbed (total, water and CT) versus time for the sweep experiment involving 45 wt% water on P-47 particles.

If the basis for Fig. 13 is correct, it can be concluded that the total residual mass is mostly water for this experiment. The estimated water residual mass is about 10 mg/g, a 33 % reduction compared with a pure water run on these particles. The conclusion would be that the presence of CT facilitates removal of water from the particles, resulting in a lower water residual mass. The estimated CT residual mass is about 1.6 mg/g, slightly lower than the 2.3 mg/g value found for pure CT on these particles. Since the CT residual mass is sensitive to assumptions about the initial removal rates, the estimated value on Fig. 13 should be considered only an approximation.

ACKNOWLEDGMENTS

The authors would like to thank the Environmental Management Science Program of the Office of Science, U.S. Department of Energy for financial support under grant DE-FG07-02ER63503, the Center for Applied Thermodynamic Studies at The University of Idaho for providing facilities and equipment for a portion of this work, and Ms. Diana Washington, Mr. Oscar Marin, Mr. Matthew Mower, Ms. Jennifer Hudson, Mr. Thomas May, Dr. Zhengjun Shan, Dr. Siriluk Chiarakorn and Mr. Alma Schurig for their assistance with the project. Dr. Gary Groenewold and Dr. Jani Ingram of INEEL provided facilities and assistance relative to porous materials characterization. Dr. Robert Riley of PNNL provided guidance throughout the project. Any opinions, findings, and conclusions or recommendations expressed in this material are those of the authors and do not necessarily reflect the views of the Department of Energy.

REFERENCES

1. Beck, J.S.; Vartuli, J.C.; Roth, W.J.; Leonowicz, M.E.; Kresge, C.T.; Schmitt, K.D.; Chu, C.T-W.; Olson, D.H.; Sheppard, E.W.; McCullen, S.B.; Higgins, J.B.; Schlenker, J.L. *J. Am. Chem. Soc.* **1992**, *114*, 10834-10843.
2. Huo, Q.; Feng, J.; Schüth, F.; Stucky, G.D. *Chem. Mater.* **1997**, *9(No. 1)*, 14-17.
3. Inagaki, S.; Guan, S.; Fukushima, Y.; Ohsuna, T.; Terasaki, O. *J. Am. Chem. Soc.* **1999**, *121*, 9611-9614.
4. Zhao, D.; Huo, Q.; Feng, J.; Chmelka, F.; Stucky, G. *J. Am. Chem. Soc.* **1998**, *120*, 6024-6036.
5. Hakuman, M.; Naono, H. *J. Colloid and Interface Sci.* **2001**, *241*, 127-141.
6. Miyata, T.; Endo, A.; Ohmori, T.;Akiya, T.; Nakaiwa, M.J. *J. of Colloid and Interface Sci.* **2003**, *262*, 116-125.
7. Armstrong, J.E.; Frind, E.O.; McClellan, R.D. *Water Resources Research* **1994**, *30(No. 2)*, 335-368.
8. Unger, D.R.; Lam, T.T.; Schaefer, C.E.; Kosson, D.S. *Envir. Sci. Technol.* **1996**, *30*, 1081-1091.
9. Oh, J.S.; Shin, W.G.; Lee, J.W.; Kim, J.H.; Moon, H.; Seo, G. *J. Chem. Eng. Data* **2003,** *48*, 1458-1462.
10. Farrell, J.; Reinhard, M. *Envir. Sci. Technol.* **1994**, *28(No. 1)*, 53-72.
11. Hughes, B.M.; Gilham, R.W., Mendoza, C.A. In *Subsurface Contamination by Immiscible Fluids*; Proceedings of the International Conference on Subsurface Contamination by Immiscible Fluids; A. A. Balkema, Rotterdam, 1992; pp 81-88.
12. Weber, W.J. Jr.; LeBoeuf, E.J.; Young, T.M.; Huang, W. *Wat. Res.* **2001**, *35(No. 4)*, 853-868.
13. Gustafsson, O.; Haghseta, F.; Chan, C.; MacFarlane, J.; Gschwend, P.M. *Environ. Sci. Technol.* **1997**, *31(No. 1)*, 105-113.
14. Huang, W.; Yu, H.; Weber, W.J. Jr. *J. Contaminant Hydrology* **1998**, *31*, 129-148.
15. May, E.F.; Miller, R.C.; Shan, Z. *J. Chem. Eng. Data* **2001**, *46*, 1160-1166.
16. Lemmon, E.W.; Jacobsen, R.T.; Penoncello, S.G.; Beyerlein, S.W. *Computer Programs for Calculating Thermodynamic Properties of Fluids of Engineering Interest* **1997**, Center for Applied Thermodynamic Studies Report 97-2, University of Idaho, Moscow, ID.
17. Myers, A.L. *AIChE J.* **2002**, *48(No. 1)*, 145-160.
18. Kim, J.; Joung, K.C.; Yoo, K-P.; Bae, S.Y. *Fluid Phase Equilibria* **1998**, *150-151*, 679-686.

19. Mower, M.B. *Competitive Desorption of Carbon Tetrachloride + Water from Mesoporous Silica Paritcles* **2005**, MS Thesis, Washington State University, Pullman, WA.

20. Hudson, J. *Equilibrium and Kinetic Studies of Carbon Tetrachloride on Porous Silicas: Isotherms and the Effect of Pore Size on Desorption Rates* **2003**, MS Thesis, Washington State University, Pullman, WA.

21. May, T.O. *Fluid Properties and Adsorption Measurements: 1) Densities and Dew Points of CH_4+CO_2; 2) Competitive Adsorption for CCl_4+H_2O on Porous Silica; 3) Development and Testing of a Labview Algorithm for Fitting Complex Data to Nonlinear Functions, with Application to the Dielectric Properties of CH_4* **2003**, MS Thesis, Washington State University, Pullman, WA.

22. Chiarakorn, S. *Equilibrium Isotherms and Desorption Rate Studies of Carbon Tetrachloride on MCM-41 Synthesized from Rice Husk Silica* **2003**, Center for Multiphase Environmental Research Report, Washington State University, Pullman, WA.

23. Tanev, P.T.; Vlaev, L.T. *J. Colloid Interface Sci.* **1993**, *160*, 110-116.

24. Marin Flores, O.G. *Desorption of Carbon Tetrachloride from Mesoporous Silica Particles* **2004**, MS Thesis, Washington State University, Pullman, WA.

25. Li, J.; Werth, C.J. *Environ. Sci. Technol.* **2004**, *38*, 440-448.

26. Suyadal, Y. *Ind. Eng. Chem. Res.* **2003**, *42*, 897-903.